

# Lightweight Monocular Depth with a Novel Neural Architecture Search Method

Lam Huynh<sup>1</sup>   Esa Rahtu<sup>2</sup>   Jiri Matas<sup>3</sup>   Janne Heikkilä<sup>1</sup>

<sup>1</sup>Center for Machine Vision and Signal Analysis, University of Oulu

<sup>2</sup>Computer Vision Group, Tampere University

<sup>3</sup>Center for Machine Perception, Czech Technical University, Czech Republic

## Abstract

We present *LDP*, a lightweight dense prediction neural architecture search (NAS) framework. Starting from a pre-defined generic backbone, *LDP* applies the novel Assisted Tabu Search for efficient architecture exploration. *LDP* is fast and suitable for various dense estimation problems, unlike previous NAS methods that are either computational demanding or deployed only for a single subtask. The performance of *LDP* is evaluated on monocular depth estimation, semantic segmentation, and image super-resolution tasks on diverse datasets, including *NYU-Depth-v2*, *KITTI*, *Cityscapes*, *COCO-stuff*, *DIV2K*, *Set5*, *Set14*, *BSD100*, *Urban100*. Experiments show that the proposed framework yields consistent improvements on all tested dense prediction tasks, while being 5% – 315% more compact in terms of the number of model parameters than prior arts.

Dense prediction is a class of computer vision problems aiming at mapping every pixel of the input image with some predicted values. Depending on the problem, the output values can be either continuous or discrete. For instance, monocular depth estimation and image super-resolution are often formulated as regression, while semantic segmentation is a dense classification, i.e. discrete, problem. More specifically, the monocular depth estimation problem produces a dense depth map from a single image to be used in various applications including robotics, scene understanding, and augmented reality. Single image super-resolution (SISR) is a low-level vision task that generates a high-resolution image from its low-resolution counterpart. SISR is widely utilized in medical and surveillance imaging, where images with more precise details can provide invaluable information. On the other hand, semantic segmentation predicts a dense annotated map of different semantic categories from a given image that is crucial for image understanding tasks.

Recent deep neural networks (DNN) exhibits remarkable results on dense prediction, especially subproblems such as single image depth estimation [10, 17, 31, 47, 52, 62, 69,

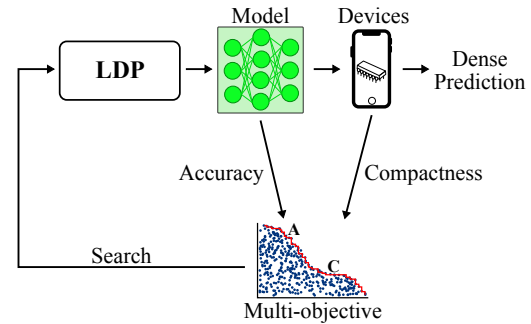


Figure 1. The proposed framework enables efficient NAS for various lightweight dense prediction tasks including depth prediction, semantic segmentation and image super-resolution.

70, 82, 98, 15, 63, 83, 33, 37], semantic segmentation [44, 16, 65, 78, 95, 104], and single image super-resolution [24, 8, 92].

Nonetheless, state-of-the-art methods mainly enhance dense prediction accuracy by increasing network complexity hindering the applicability on resource limited devices. Vision transformer-based approaches [83, 98, 73, 54] achieve state-of-the-art results but are subservient to large model and massive data from training.

The most straightforward way to deal with the computational limitations is to use simple and small architectures [96]. Usually such simple designs are unreliable and yield low-quality predictions. Other popular strategies include quantizing the weights of a network into low-precision fixed-point operations [40] or pruning by directly cutting off less important filters [99]. Nevertheless, these methods depend on a baseline model, tend to degrade their performance afterwards and are incapable of exploring new combinations of DNN operations. Moreover, creating a resource-constrained model is a non-trivial task requiring 1) expert knowledge to carefully balance accuracy and resources and 2) plenty of tedious trial-and-error work.

Neural architecture search (NAS), proposed recently [113, 114], exhibits compelling results, and more importantly, promises to release from manual tweaking of deep neural architectures. Unfortunately, NAS methods

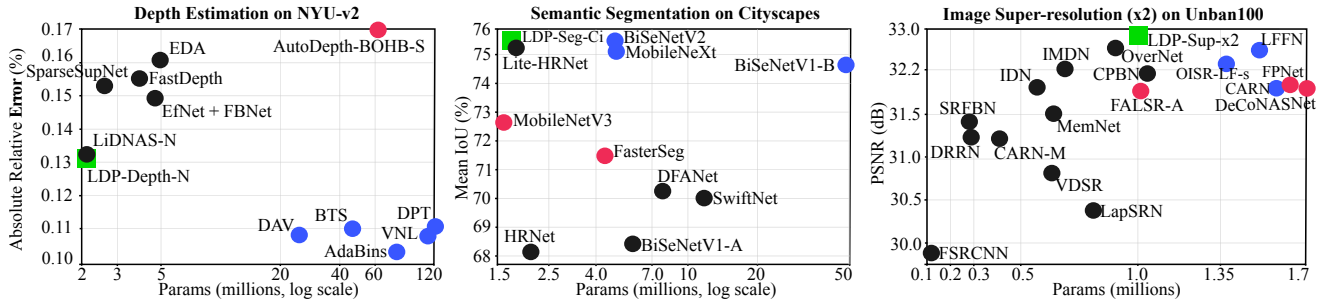


Figure 2. From left to right, absolute relative error, mean intersection-over-union and peak signal-to-noise ratio vs. the number of parameters for recent dense prediction methods on NYU-Depth-v2 (left), Cityscapes (middle) and Urban100 (right) – the LDP models outperforms the lightweight baselines (black), while using substantially less parameters than the current state-of-the-art methods (blue). Compared to the recent NAS-based approaches (red), LDP improves in both performance and compactness.

mostly require thousands of training hours on hundreds of GPUs. To address this, recent NAS studies introduced various techniques to increase the efficiency, including weight sharing [79], and network transformation [28]. These methods show promising results, but they are still expensive and mainly focus on classification and detection.

This paper introduces LDP, which is a novel multi-objective NAS framework, capable of searching for accurate and lightweight dense prediction architectures as shown in Figure 1. The approach is based on three core ideas. First, the previous NAS methods essentially search for a few types of cells and then repeatedly accumulate the same cells to build the whole network. Although doing this simplifies the search process, it also restrains layer diversity that is important for computational efficiency. On the other hand, multi-scale pyramid network structure has been successful for many dense prediction tasks including optical flow [90], depth estimation [80], semantic segmentation [109], and image super-resolution [3]. Based on these observations, we construct a generic pre-defined backbone network that utilizes different layers striving for the right balance between flexibility and search space size.

Second, we propose the Assisted Tabu Search (ATS) for efficient neural architecture search. Inspired by the recent NAS study that suggests estimating network performance without training [76], we integrate this idea into our multi-objective search function to swiftly evaluate our candidate networks. This, in turn, significantly reduces search time compared to state-of-the-art NAS-based approaches [86, 16, 30].

Third, most NAS studies tied architecture search to a single task, either semantic segmentation [16] or depth estimation [86, 51] or image super-resolution [30]. By utilizing ATS together with a generic pre-defined backbone, LDP generalizes architecture search for various dense prediction problems.

Figure 2 presents a comparison between our LDP models and other state-of-the-art lightweight approaches for monocular depth estimation, semantic segmentation and

image super-resolution tasks. Compared to PyD-Net [80], our method improves the REL, RMSE, and thresholded accuracy by 13.6%, 8.3%, and 3% with similar execution time on the Google Pixel 3a phone (see Table 7). Compared to FastDepth [96] and EDA [94], our model achieves higher accuracy with fewer parameters.

To summarize, our work makes the following contributions:

- We propose a multi-objective exploration framework, LDP, searching for accurate and lightweight dense prediction architectures. It extends our previous work [51] on monocular depth estimation to multiple prediction problems.
- We leverage the novel Assisted Tabu Search to enable fast neural architecture search.
- We create a well-defined search space that allows computational flexibility and layer diversity.
- We achieve state-of-the-art results compared to lightweight baselines on diverse problems and datasets, with significantly less parameters.

The implementation of LDP will be made publicly available upon publication of the paper.

## 1. Related work

**Dense prediction problem** We focus on three dense prediction subtasks: such as monocular depth estimation, semantic segmentation and image super-resolution.

Learning-based monocular depth estimation was first introduced by Saxena et al. [88]. Later studies improved accuracy by using large network architectures [17, 26, 27, 47, 61] or integrating semantic information [55] and surface normals [81]. Fu et al. [32] formulated depth estimation as an ordinal regression problem, while [15, 63] estimated relative instead of metric depth. Facil et al. [31] proposed to learn camera calibration from the images for depth estimation. Recent approaches further improve the performance by exploiting monocular priors such as planarity constraints [69, 70, 101, 52, 62] or occlusion [82]. Gonzalez

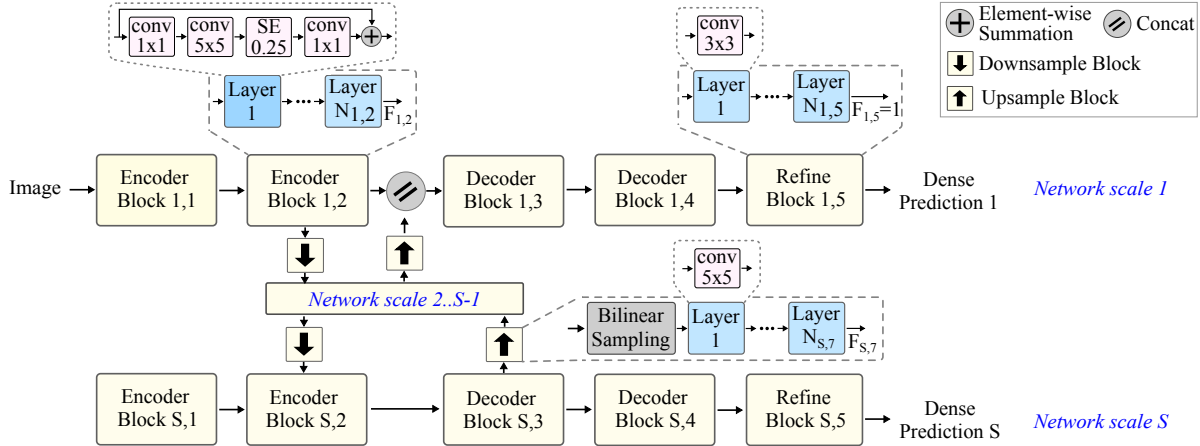


Figure 3. The search space of our LDP framework. Models are constructed from a pre-defined backbone network containing encoder, decoder, refine, downsample and upsample blocks (green). A block is formed by several identical layers (orange) that are generated from a pool of operations and connections. Layers within a block are the same while layers of different blocks can be different.

and Kim [38] estimated depth by synthesizing stereo pairs from a single image, while [98] and [83] applied vision-transformer for depth prediction. For resource-limited hardware, it is more desirable to not only have a fast but also accurate model. A simple alternative is employing lightweight architectures such as MobileNet [44, 45, 87, 96], GhostNet [39], and FBNet [94]. A popular approach is utilizing network compression techniques, including quantization [40], network pruning [99], knowledge distillation [105]. Another approach employs well-known pyramid networks or dynamic optimization schemes [4].

Deep neural networks have thrived on semantic segmentation, with early works [35, 41] proposed to classify region proposals to perform this task. Later on, fully convolutional neural network methods [74, 21] are widely adopted to process arbitrary-sized input images and train the network end-to-end. Atrous convolution-based approach [68] generated the middle-score map that was later refined using the dense conditional random field (CRF) [59] to mitigate the low-resolution prediction problem. Chen et al. [12] then implemented atrous spatial pyramid pooling for segmenting objects at different scales, while [13] and [14] employed atrous separable convolution and an efficient decoder module to capture sharp object boundaries. Zheng et al. [110] enabled end-to-end training of dense CRF by implementing recurrent layers. Other approaches [6, 77] utilized transposed convolution to generate the high-resolution prediction. Long et al. [74] produced multi-resolution prediction scores and took the average to generate the final output. Hariharan et al. [42] fused mid-level features and trained dense classification layers at multiple stages. Badrinarayanan et al. [6] and Ronneberger et al. [85] implemented transposed convolution with skip-connections to exploit mid-level features. Wang et al. [95] utilized multi-scale parallel inter-connected layers to further exploit learned features from pre-trained ImageNet models.

Lightweight approaches [78, 65, 103] employed pre-trained backbones as a decoder and a simple decoder to perform fast segmentation. Zhao et al. [108] modified the cascade architecture of [109] to shrink the model size and speed-up inference.

Image super-resolution task has also been immensely improved using deep neural networks. Dong et al. [23] first proposed a shallow but bulky network that [24] later shrunk down utilizing transposed convolution. Kim et al. [56] implemented a deeper architecture with skip connection while Zhang et al. [107] proposed channel attention to improve the performance. Kim et al. [57] introduced recursive layers that Tai et al. [91] later extended by adding the local residual connection. Likewise, many studies attempted to enhance model efficiency. Ahn et al. [3] suggested using cascade architecture and group convolution to reduce the number of parameters. Hui et al. [50, 49] proposed the information distillation module for creating an efficient model. Lai et al. [60] applied the Laplacian pyramid network to gradually increase the spatial resolution while downsizing the model.

However, state-of-the-art methods mainly focus on increasing accuracy at the cost of model complexity that is infeasible in resource-limited settings, while manually designed lightweight architecture is a tedious task, requires much trial-and-error, and usually leads to architectures with low accuracy.

**Neural Architecture Search** There has been increasing interest in automating network design using neural architecture search. Most of these methods focus on searching high-performance architecture using reinforcement learning [7, 71, 79, 113, 114], evolutionary search [84], differentiable search [72], or other learning algorithms [75]. However, these methods are usually very slow and require huge resources for training. Other studies [25, 29, 46] also attempt to optimize multiple objectives like model size and accuracy. Nevertheless, their search process optimizes

only on small tasks like CIFAR. In contrast, our proposed method targets real-world data such as NYU, KITTI, and Cityscapes on multiple dense prediction tasks.

## 2. Lightweight Dense Precition (LDP)

We propose the LDP framework to search for accurate and lightweight monocular depth estimation architectures utilizing a pre-defined backbone that has been successful for dense prediction in the past. The proposed framework takes in a dataset as input to search for the best possible model. This model can be deployed for depth estimation on hardware-limited devices. The first subsection defines the search space while the remaining two describe our multi-objective exploration and search algorithm.

### 2.1. Search Space

Previous neural architecture search (NAS) studies demonstrated the significance of designing a well-defined search space. A common choice of NAS is searching for a small set of complicated cells from a smaller dataset [114, 71, 84]. These cells are later replicated to construct the entire architecture that hindered layer diversity and suffered from domain differences [93]. On the other hand, unlike classification tasks, dense prediction problems involve mapping a feature representation in the encoder to predictions at larger spatial resolution in the decoder.

To this end, we build our search space upon a pre-defined backbone that is shown as the set of green blocks in Figure 3. The backbone is divided into multi-scale pyramid networks operating at different spatial resolutions. Each network scale consists of two encoder blocks, two decoder blocks, a refinement block, a downsampling and upsampling block (except for scale 1). Each block is constructed from a set of identical layers (marked as orange in Figure 3). Inspired by [93], we search for the layer from a pool of operations and connections, including:

- The number of resolution scales  $S$ .
- The number of layers for each block  $N_{i,j}$ .
- Convolutional operations (ConvOps): vanilla 2D convolution, depthwise convolution, inverted bottleneck convolution and micro-blocks [66].
- Convolutional kernel size (KSize):  $3 \times 3, 5 \times 5$ .
- Squeeze and excitation ratio (SER): 0, 0.25.
- Skip connections (SOps): residual or no connection.
- The number of output channels:  $F_{i,j}$ .

Here  $i$  indicates the resolution scale and  $j$  is the block index at the same resolution. Internal operations such as ConvOps, KSize, SER, SOps,  $F_{i,j}$  are utilized to construct the layer while  $N_{i,j}$  determines the number of layers that will be replicated for block  $i,j$ . In other words, as shown in Figure 3, layers within a block (e.g. layers 1 to  $N_{1,2}$  of Encoder Block 1,2 are the same) are similar while layers of different

blocks (e.g. Layer 1 in Refine Block 1,5 versus Layer 1 in Upsample Block S,7) can be different.

We also perform layer mutation to further diversifying the network structure during the architecture search process. The mutation operations include:

- Swapping operations of two random layers with compatibility check.
- Modifying a layer with a new valid layer from the pre-defined operations.

Moreover, we also set computational constraints to balance the kernel size with the number of output channels. Therefore, increasing the kernel size of one layer usually results in decreasing output channels of another layer.

Assuming we have a network of  $S$  scales, and each block has a sub-search space of size  $M$  then our total search space will be  $M^{5+[(S-1)*7]}$ . Supposedly, a standard case with  $M = 192, S = 5$  will result in a search space of size  $\sim 2 \times 10^{75}$ .

### 2.2. Multi-Objective Exploration

We introduce a multi-objective search paradigm seeking for both accurate and compact architectures. For this purpose, we monitor the *validation grade*  $\mathcal{G}$  that formulates both accuracy and the number of parameter of the trained model. It is defined by

$$\mathcal{G}(m) = \alpha \times A(m) + (1 - \alpha) \times \left[ \frac{P}{P(m)} \right]^r \quad (1)$$

where  $A(m)$  and  $P(m)$  are validation accuracy and the number of parameters of model  $m$ .  $P$  is the target compactness,  $\alpha$  is the balance coefficient, and  $r$  is an exponent with  $r = 0$  when  $P(m) \leq P$  and otherwise  $r = 1$ . The goal is to search for an architecture  $m^*$  where  $G(m^*)$  is maximum.

However, computing  $G$  requires training for every architecture candidate, resulting in considerable search time. To mitigate this problem, Mellor et al. [76] suggested to score an architecture at initialisation to predict its performance before training. For a network  $f$ , the *score*( $f$ ) is defined as:

$$\text{score}(f) = \log|K_H| \quad (2)$$

where  $K_H$  is the kernel matrix. Let us assume that the mapping of model  $f$  from a batch of data  $X = \{x_i\}_{i=1}^N$  is  $f(x_i)$ . By assigning binary indicators to every activation units in  $f$ , a linear region  $x_i$  of data point  $i$  is represented by the binary code  $c_i$ . The kernel matrix  $K_H$  is defined as:

$$K_H = \begin{pmatrix} N_A - d_H(c_1, c_1) & \dots & N_A - d_H(c_1, c_N) \\ \vdots & \ddots & \vdots \\ N_A - d_H(c_N, c_1) & \dots & N_A - d_H(c_N, c_N) \end{pmatrix} \quad (3)$$



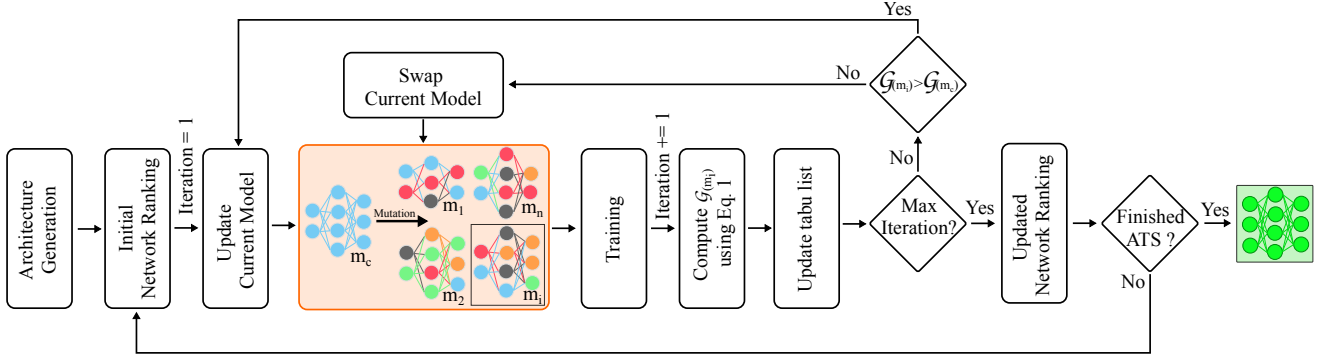


Figure 4. The flowchart of our architecture search that utilizes the Assisted Tabu Search (ATS) with mutation to search for accurate and lightweight monocular depth estimation networks.

where  $N_A$  is the number of activation units, and  $d_H(c_i, c_j)$  is the Hamming distance between two binary codes. Inspired by this principle, we generate and train a set of different architectures for various dense prediction tasks. We evaluate the performance of these models and visualize the results against the *score* that in our case is the mapping of depth values within image batches. Leveraging this observation, we 1) utilize the *score* in our initial network ranking, and 2) define the mutation exploration reward  $\mathcal{R}$  as:

$$\mathcal{R}(m_i, m_j) = \alpha \times \frac{\text{score}(m_j)}{\text{score}(m_i)} + (1 - \alpha) \times \left[ \frac{P}{P(m_j)} \right]^r \quad (4)$$

where  $m_j$  is a child network that is mutated from  $m_i$  architecture.

### 2.3. Search Algorithm

The flowchart of our architecture search is presented in Figure 4. We first randomly generate 60K unique parent models and create the initial network ranking based on the *score* in Eq. 2. We then select *six* architectures in which *three* are the highest-ranked while the other *three* have the highest score of the networks with the size closest to the target compactness.

Starting from these initial networks, we strive for the best possible model utilizing Assisted Tabu Search (ATS), inspired by Tabu search (TS) [36] that is a high level procedure for solving multicriteria optimization problems. It is an iterative algorithm that starts from some initial feasible solutions and aims to determine better solutions while being designed to avoid traps at local minima.

We propose ATS by applying Eq. 1 and 4 to TS to speed up the searching process. Specifically, we mutate numerous children models ( $m_1, m_2, \dots, m_n$ ) from the current architecture ( $m_c$ ). The mutation exploration reward  $\mathcal{R}(m_c, m_i)$  is calculated using Eq. 4. ATS then chooses to train the mutation with the highest rewards (e.g. architecture  $m_i$  as demonstrated in Figure 4). The validation grade of this model  $\mathcal{G}(m_i)$  is calculated after the training. The performance of the chosen model is assessed by comparing  $\mathcal{G}(m_i)$

with  $\mathcal{G}(m_c)$ . If  $\mathcal{G}(m_i)$  is larger than  $\mathcal{G}(m_c)$ , then  $m_i$  is a good mutation, and we opt to build the next generation upon its structure. Otherwise, we swap to use the best option in the tabu list for the next mutation. The process stops when reaching a maximum number of iterations or achieving a terminal condition. The network ranking will be updated, and the search will continue for the remaining parent architectures.

### 2.4. Implementation Details

For searching, we directly perform our architecture exploration on the training samples of the target dataset. We set the target compactness parameter  $P$  using the previously published compact models as a guideline. We set the maximum number of exploration iterations to 100 and stop the exploration procedure if a better solution cannot be found after 10 iterations. The total search time required to find optimal architecture is  $\sim 4.3$  GPU days.

For training, we use the Adam optimizer [58] with  $(\beta_1, \beta_2, \epsilon) = (0.9, 0.999, 10^{-8})$ . The initial learning rate is  $7 * 10^{-4}$ , but from epoch 10 the learning is reduced by 5% per 5 epochs. We use a batch size of 256 and augment the input RGB and ground truth depth images using random rotations ( $[-5.0, +5.0]$  degrees), horizontal flips, rectangular window droppings, and colorization (RGB only).

## 3. Experiments

We deploy the LDP framework on dense prediction tasks: monocular depth estimation, semantic segmentation, and image super-resolution. Experiments show that LDP improved performance while using only a fraction of the number of parameters needed by the competing approaches.

### 3.1. Monocular Depth Estimation

We first demonstrate our method for monocular depth estimation that can be formulated as a dense regression problem. The main goal is to infer continuous pixel-wise depth values from a single input image. For this task, we apply LDP on the NYU-Depth-v2 [89] and KITTI [34] datasets.

Table 1. Evaluation on the NYU-Depth-v2 dataset. Metrics with  $\downarrow$  mean lower is better and  $\uparrow$  mean higher is better. Type column shows the exploration method used to obtain the model. RL, ATS, and manual, refer to reinforcement learning, assisted tabu search, and manual design, respectively.

Architecture		#params	Type	Search Time	REL $\downarrow$	RMSE $\downarrow$	$\delta_1\uparrow$	$\delta_2\uparrow$	$\delta_3\uparrow$
AutoDepth-BOHB-S	Saikia et al.'19 [86]	63.0M	RL	42 GPU days	0.170	0.599	-	-	-
EDA	Tu et al.'21 [94]	5.0M	Manual	-	0.161	0.557	0.782	0.945	0.984
Ef+FBNet	Tu & Wu et al. [94, 97]	4.7M	Manual	-	0.149	0.531	0.803	0.952	0.987
FastDepth	Wofk et al.'19 [96]	3.9M	Manual	-	0.155	0.599	0.778	0.944	0.981
SparseSupNet	Yucel et al.'21 [105]	2.6M	Manual	-	0.153	0.561	0.792	0.949	0.985
LiDNAS-N	Huynh et al.'21 [51]	2.1M	ATS	4.3 GPU days	<b>0.132</b>	0.487	0.845	0.965	<b>0.993</b>
LDP-Depth-N	Ours	<b>2.0M</b>	ATS	4.3 GPU days	<b>0.132</b>	<b>0.483</b>	<b>0.848</b>	<b>0.967</b>	<b>0.993</b>

NYU-Depth-v2 contains  $\sim 120K$  RGB-D images obtained from 464 indoor scenes. From the entire dataset, we use 50K images for training and the official test set of 654 images for evaluation. KITTI is an outdoor driving dataset, where we use the standard Eigen split [26, 27] for training (39K images) and testing (697 images). We report the mean absolute relative error (REL), root mean square error (RMSE), and thresholded accuracy ( $\delta_i$ ) as our performance metrics.

In the case of NYU-Depth-v2, we set the target compactness  $P = 1.8M$  with the balance coefficient  $\alpha = 0.6$  to search for the optimized model on NYU-Depth-v2. We then select the best performance model (LDP-Depth-N) and

Table 2. Evaluation on the KITTI dataset. Metrics with  $\downarrow$  mean lower is better and  $\uparrow$  mean higher is better.

Method	#params	REL $\downarrow$	RMSE $\downarrow$	$\delta_1\uparrow$	$\delta_2\uparrow$	$\delta_3\uparrow$
FastDepth [96]	3.93M	0.156	5.628	0.801	0.930	0.971
PyD-Net [80]	1.97M	0.154	5.556	0.812	0.932	0.970
EQPyD-Net [19]	1.97M	0.135	5.505	0.821	0.933	0.970
DSNet [4]	1.91M	0.159	5.593	0.800	0.932	0.971
LiDNAS-K	1.78M	<b>0.133</b>	5.157	0.842	<b>0.948</b>	0.980
LDP-Depth-K	<b>1.74M</b>	<b>0.133</b>	<b>5.155</b>	<b>0.844</b>	<b>0.948</b>	<b>0.981</b>

Table 3. Segmentation results on Cityscapes dataset. (MIoU)

Model	#params	resolution	val $\uparrow$	test $\uparrow$
BiSeNetV1 B [103]	49.0M	768 $\times$ 1536	74.8	74.7
SwiftNet[78]	11.8M	512 $\times$ 1024	70.2	-
DFANet [65]	7.8M	512 $\times$ 1024	70.8	70.3
BiSeNetV1 A [103]	5.8M	768 $\times$ 1536	69.0	68.4
MobileNeXt [111]	4.5M	1024 $\times$ 2048	75.5	75.2
BiSeNetV2 [102]	4.3M	1024 $\times$ 2048	75.8	75.3
HRNet-W16 [95]	2.0M	512 $\times$ 1024	68.6	68.1
Lite-HRNet [104]	1.8M	512 $\times$ 1024	<b>76.0</b>	75.3
FasterSeg [16]	4.4M	1024 $\times$ 2048	73.1	71.5
MobileNetV3 [44]	<b>1.5M</b>	1024 $\times$ 2048	72.4	72.6
LDP-Seg-Ci	1.7M	512 $\times$ 1024	75.8	<b>75.5</b>

Table 4. Segmentation results on COCO-Stuff dataset.

Model	#params	PixAcc(%) $\uparrow$	MIoU(%) $\uparrow$
BiSeNetV1 B [103]	49.0M	63.2	28.1
ICNet [108]	12.7M	-	29.1
BiSeNetV1 A [103]	5.8M	59.0	22.8
BiSeNetV2 [102]	<b>4.3M</b>	63.5	28.7
LDP-Seg-CO	<b>4.3M</b>	<b>64.2</b>	<b>29.3</b>

compare its results with lightweight state-of-the-art methods [94, 96, 97, 105] along with their numbers of parameters. As shown in Table 1, LDP-Depth-N outperforms the baseline while containing the least amount of parameters. Comparing with the best-performing approach, the proposed model improves the REL, RMSE, and  $\theta_1$  by 11.4%, 8.2%, and 6.8% while compressing the model size by 55%. Our method produces high-quality depth maps with sharper details as presented in Figure 11. However, we observe that all methods still struggle in challenging cases, such as the scene containing Lambertian surfaces as illustrated by the example in the third column of Figure 11. Moreover, the proposed method improves REL and RMSE by 22.3% and 18.7% while using only 3% of the model parameters comparing to the state-of-the-art NAS-based disparity and depth estimation approaches [86]. In addition, our method requires 90% less search time than [86] and outperforms [51] in almost all metrics.

For KITTI, we aim at the target compactness of  $P = 1.45M$  with  $\alpha = 0.55$ . We train our candidate architectures with the same self-supervised procedure proposed by [37] and adopted by the state-of-the-art approaches [4, 19, 80, 96]. After the search, we pick the best architecture (LDP-Depth-K) to compare with the baselines and report the performance figures in Table 2. The LDP-Depth-K model yields competitive results with the baselines while also being the smallest model. We observe that our proposed method provides noticeable improvement from PyD-Net and EQPyD-Net. Examples from Figure 8 show that the predicted depth maps from LDP-Depth-K are more accurate and contain fewer artifacts.

### 3.2. Semantic Segmentation

We then deploy LDP for dense classification tasks such as semantic segmentation that aims to predict discrete labels of image pixels. We employ the same backbone structure as in monocular depth estimation experiments and utilize the cross-entropy loss. For this problem, we evaluate our method on the Cityscapes [20] and COCO-stuff [11] datasets. Cityscapes is an outdoor dataset containing images of various urban scenarios. The dataset consists of 5K high-quality annotated frames that 19 classes are used for semantic segmentation. Following the standard procedure,

Table 5. Image Super-Resolution with scaling factor  $\times 2$ .

Method	#params	Set5		Set14		BSD100		Urban100	
		PSNR $\uparrow$	SSIM $\uparrow$	PSNR $\uparrow$	SSIM $\uparrow$	PSNR $\uparrow$	SSIM $\uparrow$	PSNR $\uparrow$	SSIM $\uparrow$
Bicubic	-	33.66	0.9299	30.24	0.8688	29.56	0.8431	26.91	0.8425
CARN [3]	1.59M	37.76	0.9590	33.52	0.9166	32.09	0.8978	31.92	0.9256
LF2N [100]	1.52M	37.95	0.9597	32.45	0.9142	32.20	0.8994	32.39	0.9299
OISR-LF-s [43]	1.37M	38.02	0.9605	33.62	0.9178	32.20	0.9000	32.21	0.9290
CBPN [112]	1.04M	37.90	0.9590	33.60	0.9171	32.17	0.8989	32.14	0.9279
OverNet [8]	0.90M	38.11	0.9610	33.71	0.9179	32.24	0.9007	32.44	0.9311
LapSRN [60]	0.81M	37.52	0.9590	33.08	0.9130	31.80	0.8950	30.41	0.9100
IMDN [49]	0.69M	38.00	0.9605	33.63	0.9177	32.19	0.8996	32.17	0.9283
MemNet [92]	0.67M	37.78	0.9597	33.28	0.9142	32.08	0.8978	31.31	0.9195
VDSR [56]	0.66M	37.53	0.9587	33.05	0.9127	31.90	0.8960	30.77	0.9141
IDN [50]	0.57M	37.85	0.9598	33.58	0.9178	32.11	0.8989	31.95	0.9266
CARN-M [3]	0.41M	37.53	0.9583	33.26	0.9141	31.92	0.8960	31.23	0.9194
DRRN [91]	0.29M	37.74	0.9591	33.23	0.9136	32.05	0.8973	31.23	0.9188
SRFBN [67]	0.28M	37.78	0.9597	33.35	0.9156	32.00	0.8970	31.41	0.9207
FSRCNN [24]	<b>0.12M</b>	37.00	0.9558	32.63	0.9088	31.53	0.8920	29.88	0.9020
DeCoNASNet [2]	1.71M	37.96	0.9594	33.63	0.9175	32.15	0.8986	32.03	0.9265
FPNet [30]	1.61M	<b>38.13</b>	<b>0.9616</b>	<b>33.83</b>	<b>0.9198</b>	<b>32.29</b>	0.9018	32.04	0.9278
FALSR-A [18]	1.03M	37.82	0.9595	33.55	0.9168	32.12	0.8987	31.93	0.9256
LDP-Sup-x2	1.02M	38.11	0.9612	<b>33.83</b>	0.9196	<b>32.29</b>	<b>0.9019</b>	<b>32.49</b>	<b>0.9314</b>

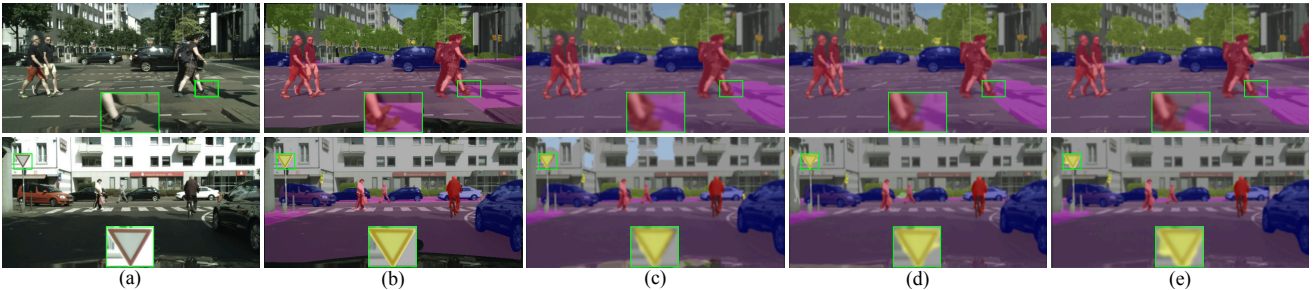


Figure 5. Comparison on the Cityscapes validation set. (a) input image, (b) ground truth, (c) LDP-Seg-Ci, (d) Lite-HRNet [104], and (e) MobileNetV3 [44].

we used 2975, 500, and 1525 images for training, validation, and testing, respectively. COCO-stuff was created by annotating dense stuffs (e.g., sky, ground, walls) from the COCO dataset. This dataset can be utilized for image understanding as it contains 91 more stuffs classes compared to the original dataset. For fair comparison, we also use the COCO-Stuff-10K with 9K and 1K for training and testing purposes. We utilize both the mean Intersection-over-Union (MIoU) as well as the pixel accuracy (pixAcc) to assess the performance of our models.

To perform searching on Cityscapes dataset, we set the target compactness  $P = 1.25M$  with the balance coefficient  $\alpha = 0.6$  using input image resolution of  $512 \times 1024$  for all experiments. We then compare the best-performing model (LDP-Seg-Ci) with recent approaches [103, 65, 78, 104, 16, 44]. Results in Table 3 suggest that LDP-Seg-Ci performs on par with state-of-the-art while using fewer pa-

rameters than most methods. Although operating at a lower resolution, our generated model outperforms FasterSeg [16] while being 61% more compact in terms of the number of parameters. Moreover, LDP-Seg-Ci also shows clear improvements compared to the MobileNetV3 [44] model. Qualitative results in Figure 5 also show that our model tends to produce more clean with sharper object boundaries and less cluttering than state-of-the-art approaches.

In the case of the COCO-stuff, we aim at the target compactness of  $P = 4.0M$  with the balance coefficient  $\alpha$  set to 0.6. During searching and testing, we crop the input into  $640 \times 640$  resolution. We evaluate the performance of our best architecture (LDP-Seg-CO) with current state-of-the-art methods [103, 108, 102] and report the results in Table 4. Our method also achieves good performance for semantic segmentation on the COCO-stuff dataset while using much fewer parameters than competing approaches.

Table 6. Image Super-Resolution with scaling factor  $\times 4$ .

Method	#params	Set5		Set14		BSD100		Urban100	
		PSNR $\uparrow$	SSIM $\uparrow$	PSNR $\uparrow$	SSIM $\uparrow$	PSNR $\uparrow$	SSIM $\uparrow$	PSNR $\uparrow$	SSIM $\uparrow$
Bicubic	-	28.42	0.8104	26.01	0.7027	25.96	0.6675	23.17	0.6585
s-LWSR64 [64]	2.27M	32.28	0.8960	28.34	0.7800	27.61	0.7380	26.19	0.7910
CARN [3]	1.59M	32.13	0.8937	28.60	0.7806	27.58	0.7349	26.07	0.7837
LFFN [100]	1.53M	32.15	0.8945	28.32	0.7810	27.52	0.7377	26.24	0.7902
OISR-LF-s [43]	1.52M	32.14	0.8947	28.63	0.7819	27.60	0.7369	26.17	0.7888
CBPN [112]	1.19M	32.21	0.8944	28.63	0.7813	27.58	0.7356	26.14	0.7869
LapSRN [60]	0.81M	31.54	0.8850	28.19	0.7720	27.32	0.7280	25.21	0.7560
IMDN [49]	0.72M	32.21	0.8948	28.58	0.7811	27.56	0.7353	26.04	0.7838
MemNet [92]	0.67M	31.74	0.8893	28.26	0.7723	27.40	0.7281	25.50	0.7630
VDSR [56]	0.66M	31.33	0.8838	28.02	0.7678	27.29	0.7252	25.18	0.7525
IDN [50]	0.60M	31.99	0.8928	28.52	0.7794	27.52	0.7339	25.92	0.7801
s-LWSR32 [64]	0.57M	32.04	0.8930	28.15	0.7760	27.52	0.7340	25.87	0.7790
SRFBN [67]	0.48M	31.98	0.8923	28.45	0.7779	27.44	0.7313	25.71	0.7719
CARN-M [3]	0.41M	31.92	0.8903	28.42	0.7762	27.44	0.7304	25.62	0.7694
DRRN [91]	0.29M	31.68	0.8888	28.21	0.7720	27.38	0.7284	25.44	0.7638
FSRCNN [24]	<b>0.12M</b>	30.71	0.8657	27.59	0.7535	26.98	0.7150	24.62	0.7280
FPNet [30]	1.61M	<b>32.32</b>	0.8962	<b>28.78</b>	<b>0.7856</b>	27.66	<b>0.7394</b>	26.09	0.7850
LDP-Sup-x4	1.09M	32.30	<b>0.8963</b>	28.54	0.7836	<b>27.67</b>	<b>0.7394</b>	<b>26.25</b>	<b>0.7927</b>

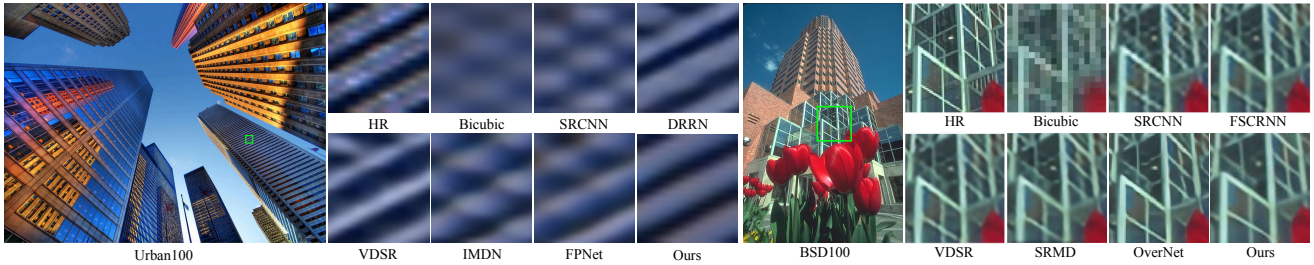


Figure 6. Comparison on the Urban100 and BSD100 dataset.

### 3.3. Image Super-resolution

To further assess the applicability of our proposed framework for dense prediction problems, we apply LDP framework for the image super-resolution task. We also employ a similar scheme as in previous experiments with added up-sample blocks between decoder and refinement blocks to increase spatial dimension within the network scale. We then perform architecture search and training on the DIV2K [1] dataset. DIV2K is a high-quality image super-resolution dataset consisting of 800 samples for training, 100 for validation, and 100 for testing purposes. After that, we test our generated models on standard benchmarks such as Set5 [9], Set14 [106], B100 [5], and Urban100 [48]. The results of our method are evaluated using the peak signal-to-noise ratio (PSNR) and structural similarity index (SSIM) metrics on the Y channel of the YCbCr color space.

We search for optimized models at super-resolution scales  $\times 2$  and  $\times 4$  on the DIV2K dataset. In both cases, we determine the target compactness of  $P = 0.8$  with the balance coefficient  $\alpha = 0.55$ . We then compare the best-

performing architectures (LDP-Sup-x2 and LDP-Sup-x4) with recent methods [30, 2, 3, 49, 18, 60] on various testing benchmarks. Tables 10 and 11 show that our models produce more competitive results than several state-of-the-art image super-resolution methods while being relatively compact. Our models perform on par with FPNet while be-

Table 7. Average runtime comparison of the proposed method and other lightweight models. Runtime values are measured using a Pixel 3a phone with input image resolution ( $640 \times 480$ ).

Architecture	CPU(ms)
Ef+FBNet [94, 97]	852
FSRCNN [24]	789
FastDepth [96]	458
VDSR [56]	425
PyD-Net [80]	226
Lite-HRNet [104]	217
LiDNAS-K [51]	205
LDP-Seg-Ci	207
LDP-Depth-K	204
LDP-Sup-x2	<b>203</b>



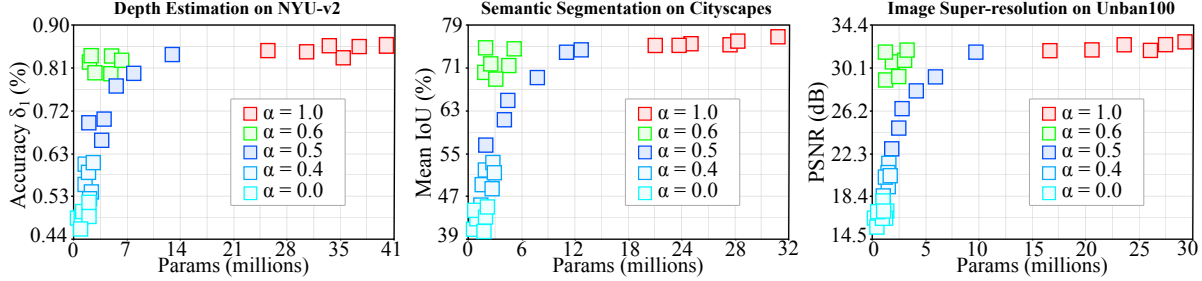


Figure 7. Trade-off between accuracy vs. the number of parameters of best models trained with different searching scenarios on NYU-Depth-v2, Cityscapes and testing on Urban100 dataset.

ing at least 32% smaller in terms of network size. Figure 10 provides visual comparisons on BSD100 and Urban100 benchmarks. The proposed method yields more accurate results than VDSR [56], DRRN [91], FSCRNN [24] and more precise details than SRCNN [22], IMDN [49], FPNNet [30] methods.

### 3.4. Runtime Measurement

We also compare the runtime of our models with state-of-the-art lightweight methods on an Android device using the app from the Mobile AI benchmark developed by Ignatov et al. [53]. To this end, we utilize the pre-trained models provided by the authors (Tensorflow [80], PyTorch [96]), convert them to *tfLite* and measure their runtime on mobile CPUs. The results in Table 7 suggest that the proposed approaches produce competing performance, with the potential of running real-time on mobile devices with further optimization.

### 3.5. Exploration Convergence

We experiment with various settings for the multi-objective balance coefficient ( $\alpha$ ) to assess its effect on the performance. For this purpose, we perform the architecture search with  $\alpha$  set to 0.0, 0.4, 0.5, 0.6, and 1.0 while the target compactness  $P = 2.0M$ . Figure 9 presents the searching progress for accuracy (left), the number of parameters (center), and validation grade (right) from one parent architecture on NYU-Depth-v2. We observe that, scenario with  $\alpha = 0.0$  quickly becomes saturated as it only gives reward to the smallest model. Searching with  $\alpha = 0.4$  favors models with compact size but also with limited accuracy. The case with  $\alpha = 0.5$  provides a more balanced option, but accuracy is hindered due to fluctuation during searching. The exploration with  $\alpha = 1.0$  seeks for the network with the best accuracy yet producing significantly larger architecture while the case where  $\alpha = 0.6$  achieves promising accuracy although with slightly bigger model than the target compactness.

### 3.6. Searching Scenarios

To further analyze the outcome of different searching scenarios, we perform architecture searches for *six* parent

networks in five settings with  $\alpha = 0.0, 0.4, 0.5, 0.6, 1.0$  and  $P = 2.0M$  on NYU-Depth-v2. Results in Figure 7 show that the best performance models in the case of  $\alpha = 0.5$  are more spread out, while training instances with  $\alpha = 0.6$

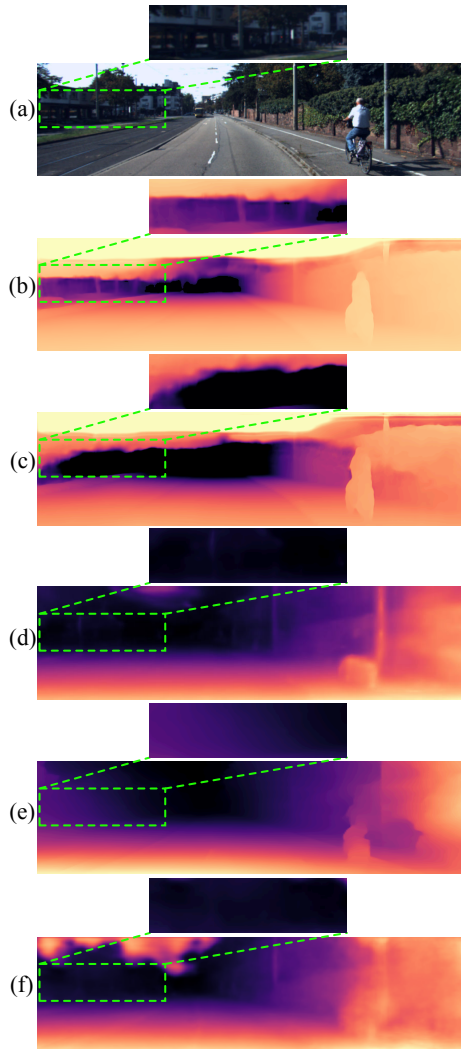


Figure 8. Comparison on the Eigen split of KITTI. (a) input image, (b) LDP-Depth-K, (c) LiDNAS-K [51], (d) DSNet [4], (e) PyD-Net [80], and (f) FastDepth [96]. Images in the right column presented zoom-in view for better visualization.

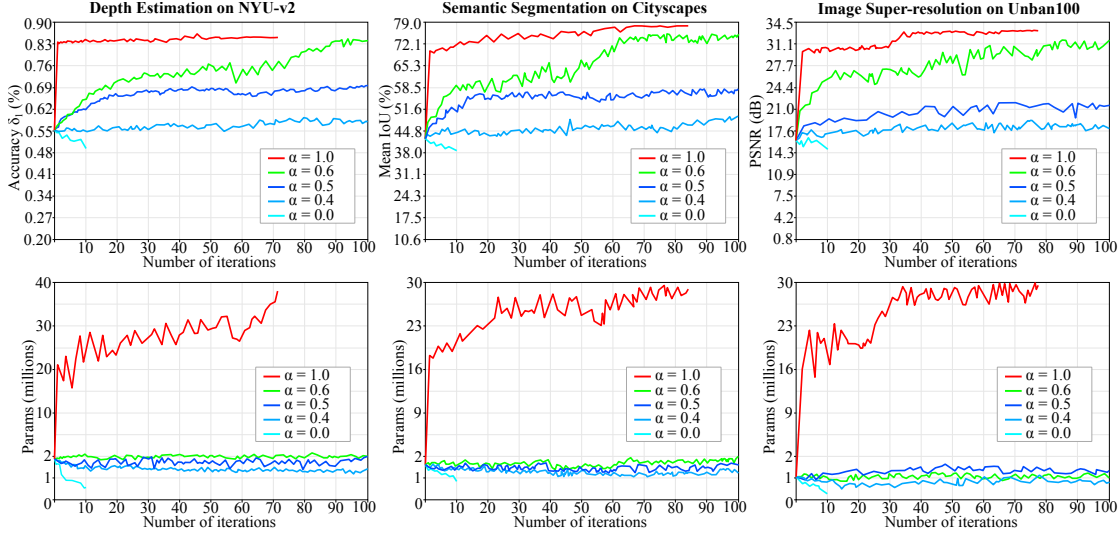


Figure 9. The progress of different searching scenarios on the NYU-Depth-v2, Cityscapes and testing on Urban100 dataset. Charts show the metrics including thresholded accuracy, Mean IoU, peak-signal-to-noise-ratio (PSNR) and the number of parameters vs. the number of searching iterations.

tend to produce both accurate and lightweight architectures. This, in turn, emphasizes the trade-off between validation accuracy and the network size.

### 3.7. Balance Coefficient Search

Determining a good balance coefficient value ( $\alpha$ ) for Eq. 1 and 4 is crucial as it greatly affects the search performance. To this end, we perform grid search on randomly subsampled sets from the training data seeking for the optimized  $\alpha$  value. The pattern in Figure 10 shows that, for NYU-Depth-v2 [4] and KITTI [2], approximately good  $\alpha$  values range from 0.5 to 0.6. Additionally, the grid search is much faster (only requires  $\sim 15$  hours on one dataset), enabling finding good  $\alpha$  values when deploying to different datasets.

## 4. Conclusion

This paper proposed a novel NAS framework to construct lightweight dense prediction architectures using Assisted Tabu Search and employing a well-defined search space for balancing layer diversity and search volume. The proposed

method achieves competitive accuracy on diverse datasets while running faster on mobile devices and being more compact than state-of-the-art handcrafted and automatically generated models. Our work provides a potential approach towards optimizing the accuracy and the network size for dense prediction without the need for manual tweaking of deep neural architectures.

## References

- [1] Eirikur Agustsson and Radu Timofte. Ntire 2017 challenge on single image super-resolution: Dataset and study. In *CVPR workshops*, pages 126–135, 2017. 8
- [2] Joon Young Ahn and Nam Ik Cho. Neural architecture search for image super-resolution using densely constructed search space: Deconas. In *2020 25th International Conference on Pattern Recognition (ICPR)*, pages 4829–4836. IEEE, 2021. 7, 8
- [3] Namhyuk Ahn, Byungkon Kang, and Kyung-Ah Sohn. Fast, accurate, and lightweight super-resolution with cascading residual network. In *Proceedings of the European Conference on Computer Vision (ECCV)*, pages 252–268, 2018. 2, 3, 7, 8
- [4] Filippo Aleotti, Giulio Zaccaroni, Luca Bartolomei, Matteo Poggi, Fabio Tosi, and Stefano Mattocchia. Real-time single image depth perception in the wild with handheld devices. *Sensors*, 21(1):15, 2021. 3, 6, 9
- [5] Pablo Arbelaez, Michael Maire, Charless Fowlkes, and Jitendra Malik. Contour detection and hierarchical image segmentation. *IEEE transactions on pattern analysis and machine intelligence*, 33(5):898–916, 2010. 8
- [6] Vijay Badrinarayanan, Alex Kendall, and Roberto Cipolla. Segnet: A deep convolutional encoder-decoder architecture for image segmentation. *IEEE transactions on pat-*

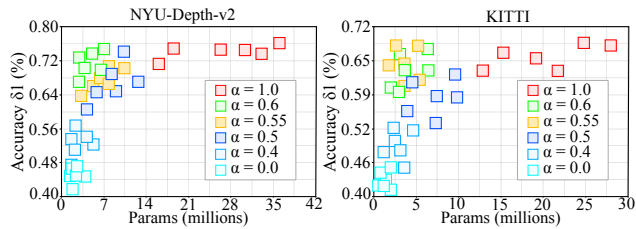


Figure 10. Grid search using randomly subsampled sets from the training data to look for good balance coefficient values on NYU-Depth-v2 (left) and KITTI (right).

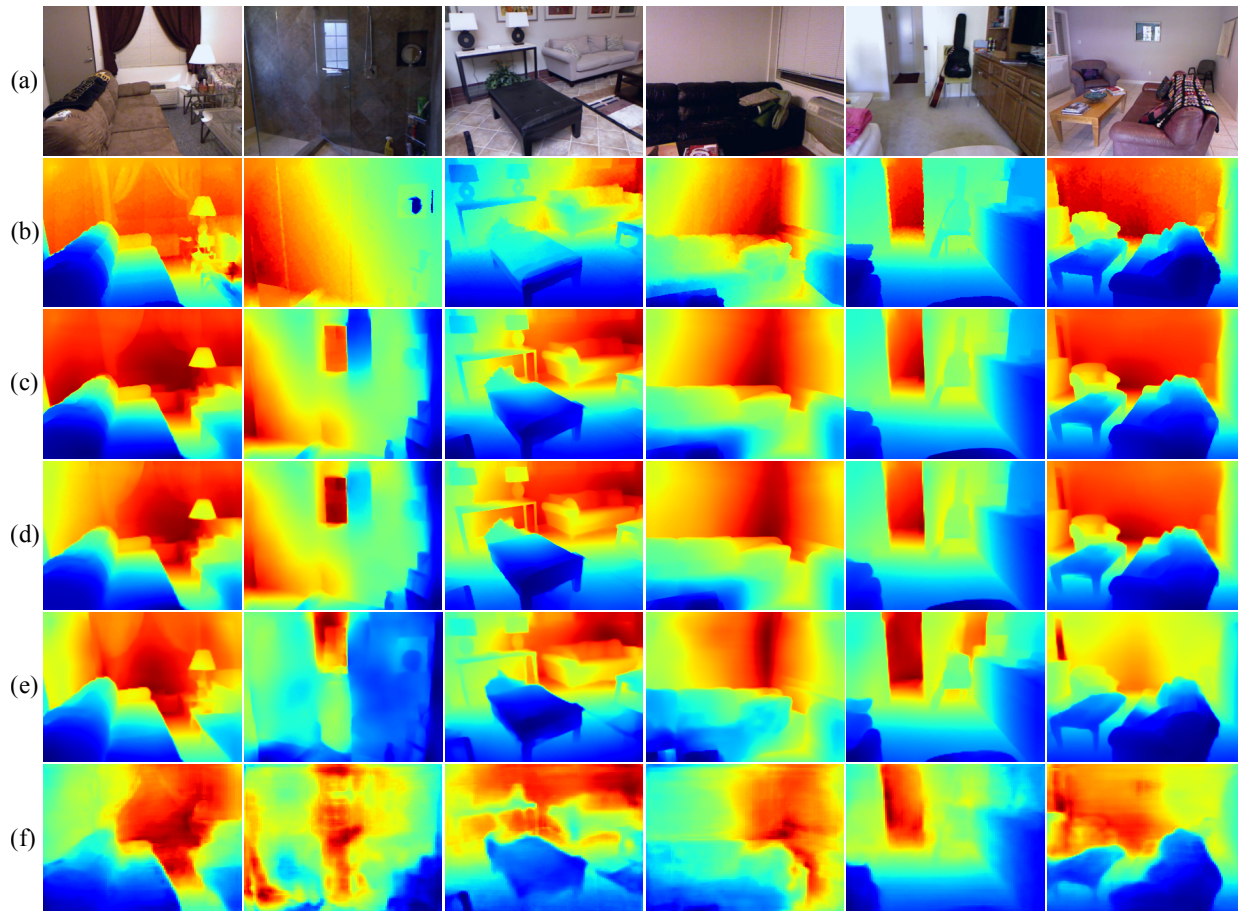


Figure 11. Comparison on the NYU test set. (a) input image, (b) ground truth, (c) LDP-Depth-N, (d) LiDNAS-N [51], (e) Ef+FBNet [94, 97], and (f) FastDepth [96].

- tern analysis and machine intelligence*, 39(12):2481–2495, 2017. 3
- [7] Bowen Baker, Otkrist Gupta, Nikhil Naik, and Ramesh Raskar. Designing neural network architectures using reinforcement learning. *arXiv preprint arXiv:1611.02167*, 2016. 3
- [8] Parichehr Behjati, Pau Rodriguez, Armin Mehri, Isabelle Hupont, Carles Fernandez Tena, and Jordi Gonzalez. Over-net: Lightweight multi-scale super-resolution with over-scaling network. In *Proceedings of the IEEE/CVF Winter Conference on Applications of Computer Vision*, pages 2694–2703, 2021. 1, 7
- [9] Marco Bevilacqua, Aline Roumy, Christine Guillemot, and Marie Line Alberi-Morel. Low-complexity single-image super-resolution based on nonnegative neighbor embedding. *British Machine Vision Conference (BMVC)*, 2012. 8
- [10] Shariq Farooq Bhat, Ibraheem Alhashim, and Peter Wonka. Adabins: Depth estimation using adaptive bins. In *Proceedings of the IEEE conference on computer vision and pattern recognition*, pages 4009–4018, 2021. 1
- [11] Holger Caesar, Jasper Uijlings, and Vittorio Ferrari. Coco-stuff: Thing and stuff classes in context. In *CVPR*, pages 1209–1218, 2018. 6
- [12] Liang-Chieh Chen, George Papandreou, Iasonas Kokkinos, Kevin Murphy, and Alan L Yuille. Deeplab: Semantic image segmentation with deep convolutional nets, atrous convolution, and fully connected crfs. *IEEE transactions on pattern analysis and machine intelligence*, 40(4):834–848, 2017. 3
- [13] Liang-Chieh Chen, George Papandreou, Florian Schroff, and Hartwig Adam. Rethinking atrous convolution for semantic image segmentation. *arXiv preprint arXiv:1706.05587*, 2017. 3
- [14] Liang-Chieh Chen, Yukun Zhu, George Papandreou, Florian Schroff, and Hartwig Adam. Encoder-decoder with atrous separable convolution for semantic image segmentation. In *Proceedings of the European conference on computer vision (ECCV)*, pages 801–818, 2018. 3
- [15] Weifeng Chen, Zhao Fu, Dawei Yang, and Jia Deng. Single-image depth perception in the wild. *Advances in neural information processing systems*, 29:730–738, 2016. 1, 2
- [16] Wuyang Chen, Xinyu Gong, Xianming Liu, Qian Zhang, Yuan Li, and Zhangyang Wang. Fasterseg: Searching for faster real-time semantic segmentation. *arXiv preprint arXiv:1912.10917*, 2019. 1, 2, 6, 7
- [17] Xiaotian Chen, Xuejin Chen, and Zheng-Jun Zha. Structure-aware residual pyramid network for monocular



- depth estimation. In *Proceedings of the 28th International Joint Conference on Artificial Intelligence*, pages 694–700. AAAI Press, 2019. 1, 2
- [18] Xiangxiang Chu, Bo Zhang, Hailong Ma, Ruijun Xu, and Qingyuan Li. Fast, accurate and lightweight super-resolution with neural architecture search. In *2020 25th International Conference on Pattern Recognition (ICPR)*, pages 59–64. IEEE, 2021. 7, 8
- [19] Antonio Cipolletta, Valentino Peluso, Andrea Calimera, Matteo Poggi, Fabio Tosi, Filippo Aleotti, and Stefano Mattoccia. Energy-quality scalable monocular depth estimation on low-power cpus. *IEEE Internet of Things Journal*, 2021. 6
- [20] Marius Cordts, Mohamed Omran, Sebastian Ramos, Timo Rehfeld, Markus Enzweiler, Rodrigo Benenson, Uwe Franke, Stefan Roth, and Bernt Schiele. The cityscapes dataset for semantic urban scene understanding. In *Proceedings of the IEEE conference on computer vision and pattern recognition*, pages 3213–3223, 2016. 6
- [21] Jifeng Dai, Kaiming He, and Jian Sun. Boxsup: Exploiting bounding boxes to supervise convolutional networks for semantic segmentation. In *Proceedings of the IEEE international conference on computer vision*, pages 1635–1643, 2015. 3
- [22] Chao Dong, Chen Change Loy, Kaiming He, and Xiaoou Tang. Learning a deep convolutional network for image super-resolution. In *European conference on computer vision*, pages 184–199. Springer, 2014. 9
- [23] Chao Dong, Chen Change Loy, Kaiming He, and Xiaoou Tang. Image super-resolution using deep convolutional networks. *IEEE transactions on pattern analysis and machine intelligence*, 38(2):295–307, 2015. 3
- [24] Chao Dong, Chen Change Loy, and Xiaoou Tang. Accelerating the super-resolution convolutional neural network. In *European conference on computer vision*, pages 391–407. Springer, 2016. 1, 3, 7, 8, 9
- [25] Jin-Dong Dong, An-Chieh Cheng, Da-Cheng Juan, Wei Wei, and Min Sun. Dpp-net: Device-aware progressive search for pareto-optimal neural architectures. In *Proceedings of the European Conference on Computer Vision (ECCV)*, pages 517–531, 2018. 3
- [26] David Eigen and Rob Fergus. Predicting depth, surface normals and semantic labels with a common multi-scale convolutional architecture. In *Proceedings of the IEEE International Conference on Computer Vision*, pages 2650–2658, 2015. 2, 6
- [27] David Eigen, Christian Puhrsch, and Rob Fergus. Depth map prediction from a single image using a multi-scale deep network. In *Advances in neural information processing systems*, pages 2366–2374, 2014. 2, 6
- [28] Thomas Elsken, Jan Hendrik Metzen, and Frank Hutter. Efficient multi-objective neural architecture search via lamarckian evolution. *arXiv preprint arXiv:1804.09081*, 2018. 2
- [29] Thomas Elsken, Jan Hendrik Metzen, and Frank Hutter. Multi-objective architecture search for cnns. *arXiv preprint arXiv:1804.09081*, 2, 2018. 3
- [30] Alireza Esmaeilzahi, M Omair Ahmad, and MNS Swamy. Fpnet: A deep light-weight interpretable neural network using forward prediction filtering for efficient single image super resolution. *IEEE Transactions on Circuits and Systems II: Express Briefs*, 2021. 2, 7, 8, 9
- [31] Jose M Facil, Benjamin Ummenhofer, Huizhong Zhou, Luis Montesano, Thomas Brox, and Javier Civera. Camconvs: camera-aware multi-scale convolutions for single-view depth. In *IEEE/CVF Conference on Computer Vision and Pattern Recognition*, pages 11826–11835, 2019. 1, 2
- [32] Huan Fu, Mingming Gong, Chaohui Wang, Kayhan Batmanghelich, and Dacheng Tao. Deep ordinal regression network for monocular depth estimation. In *CVPR*, pages 2002–2011, 2018. 2
- [33] Ravi Garg, Vijay Kumar Bg, Gustavo Carneiro, and Ian Reid. Unsupervised cnn for single view depth estimation: Geometry to the rescue. In *European conference on computer vision*, pages 740–756. Springer, 2016. 1
- [34] Andreas Geiger, Philip Lenz, Christoph Stiller, and Raquel Urtasun. Vision meets robotics: The kitti dataset. *The International Journal of Robotics Research*, 32(11):1231–1237, 2013. 5
- [35] Ross Girshick, Jeff Donahue, Trevor Darrell, and Jitendra Malik. Rich feature hierarchies for accurate object detection and semantic segmentation. In *Proceedings of the IEEE conference on computer vision and pattern recognition*, pages 580–587, 2014. 3
- [36] Fred Glover. Future paths for integer programming and links to artificial intelligence. *Computers & operations research*, 13(5):533–549, 1986. 5
- [37] Clément Godard, Oisín Mac Aodha, Michael Firman, and Gabriel J Brostow. Digging into self-supervised monocular depth estimation. In *Proceedings of the IEEE conference on computer vision and pattern recognition*, pages 3828–3838, 2019. 1, 6
- [38] Juan Luis GonzalezBello and Munchurl Kim. Forget about the lidar: Self-supervised depth estimators with med probability volumes. *Advances in Neural Information Processing Systems*, 33, 2020. 3
- [39] Kai Han, Yunhe Wang, Qi Tian, Jianyuan Guo, Chunjing Xu, and Chang Xu. Ghostnet: More features from cheap operations. In *Proceedings of the IEEE conference on computer vision and pattern recognition*, pages 1580–1589, 2020. 3
- [40] Song Han, Huizi Mao, and William J Dally. Deep compression: Compressing deep neural networks with pruning, trained quantization and huffman coding. *arXiv preprint arXiv:1510.00149*, 2015. 1, 3
- [41] Bharath Hariharan, Pablo Arbeláez, Ross Girshick, and Jitendra Malik. Simultaneous detection and segmentation. In *European conference on computer vision*, pages 297–312. Springer, 2014. 3
- [42] Bharath Hariharan, Pablo Arbeláez, Ross Girshick, and Jitendra Malik. Hypercolumns for object segmentation and fine-grained localization. In *Proceedings of the IEEE conference on computer vision and pattern recognition*, pages 447–456, 2015. 3



- [43] Xiangyu He, Zitao Mo, Peisong Wang, Yang Liu, Mingyuan Yang, and Jian Cheng. Ode-inspired network design for single image super-resolution. In *Proceedings of the IEEE conference on computer vision and pattern recognition*, pages 1732–1741, 2019. 7, 8
- [44] Andrew Howard, Mark Sandler, Grace Chu, Liang-Chieh Chen, Bo Chen, Mingxing Tan, Weijun Wang, Yukun Zhu, Ruoming Pang, Vijay Vasudevan, et al. Searching for mobilenetv3. In *Proceedings of the IEEE/CVF International Conference on Computer Vision*, pages 1314–1324, 2019. 1, 3, 6, 7
- [45] Andrew G Howard, Menglong Zhu, Bo Chen, Dmitry Kalenichenko, Weijun Wang, Tobias Weyand, Marco Andreetto, and Hartwig Adam. Mobilenets: Efficient convolutional neural networks for mobile vision applications. *arXiv preprint arXiv:1704.04861*, 2017. 3
- [46] Chi-Hung Hsu, Shu-Huan Chang, Jhao-Hong Liang, Hsin-Ping Chou, Chun-Hao Liu, Shih-Chieh Chang, Jia-Yu Pan, Yu-Ting Chen, Wei Wei, and Da-Cheng Juan. Monas: Multi-objective neural architecture search using reinforcement learning. *arXiv preprint arXiv:1806.10332*, 2018. 3
- [47] Junjie Hu, Mete Ozay, Yan Zhang, and Takayuki Okatani. Revisiting single image depth estimation: Toward higher resolution maps with accurate object boundaries. In *IEEE Winter Conf. on Applications of Computer Vision (WACV)*, 2019. 1, 2
- [48] Jia-Bin Huang, Abhishek Singh, and Narendra Ahuja. Single image super-resolution from transformed self-exemplars. In *CVPR*, pages 5197–5206, 2015. 8
- [49] Zheng Hui, Xinbo Gao, Yunchu Yang, and Xiumei Wang. Lightweight image super-resolution with information multi-distillation network. In *Proceedings of the 27th ACM International Conference on Multimedia*, pages 2024–2032, 2019. 3, 7, 8, 9
- [50] Zheng Hui, Xiumei Wang, and Xinbo Gao. Fast and accurate single image super-resolution via information distillation network. In *Proceedings of the IEEE conference on computer vision and pattern recognition*, pages 723–731, 2018. 3, 7, 8
- [51] Lam Huynh, Phong Nguyen, Jiri Matas, Esa Rahtu, and Janne Heikkilä. Lightweight monocular depth with a novel neural architecture search method. *arXiv preprint arXiv:2108.11105*, 2021. 2, 6, 8, 9, 11
- [52] Lam Huynh, Phong Nguyen-Ha, Jiri Matas, Esa Rahtu, and Janne Heikkilä. Guiding monocular depth estimation using depth-attention volume. In *European Conference on Computer Vision*, pages 581–597. Springer, 2020. 1, 2
- [53] Andrey Ignatov, Grigory Malivenko, David Plowman, Samarth Shukla, Radu Timofte, Ziyu Zhang, Yicheng Wang, Zilong Huang, Guozhong Luo, Gang Yu, et al. Fast and accurate single-image depth estimation on mobile devices, mobile ai 2021 challenge: Report. *arXiv preprint arXiv:2105.08630*, 2021. 9
- [54] Jitesh Jain, Anukriti Singh, Nikita Orlov, Zilong Huang, Jiachen Li, Steven Walton, and Humphrey Shi. Semask: Semantically masked transformers for semantic segmentation. *arXiv preprint arXiv:2112.12782*, 2021. 1
- [55] Jianbo Jiao, Ying Cao, Yibing Song, and Rynson Lau. Look deeper into depth: Monocular depth estimation with semantic booster and attention-driven loss. In *Proceedings of the European Conference on Computer Vision (ECCV)*, pages 53–69, 2018. 2
- [56] Jiwon Kim, Jung Kwon Lee, and Kyoung Mu Lee. Accurate image super-resolution using very deep convolutional networks. In *Proceedings of the IEEE conference on computer vision and pattern recognition*, pages 1646–1654, 2016. 3, 7, 8, 9
- [57] Jiwon Kim, Jung Kwon Lee, and Kyoung Mu Lee. Deeply-recursive convolutional network for image super-resolution. In *Proceedings of the IEEE conference on computer vision and pattern recognition*, pages 1637–1645, 2016. 3
- [58] Diederik P Kingma and Jimmy Ba. Adam: A method for stochastic optimization. *arXiv preprint arXiv:1412.6980*, 2014. 5
- [59] Philipp Krähenbühl and Vladlen Koltun. Efficient inference in fully connected crfs with gaussian edge potentials. *Advances in neural information processing systems*, 24:109–117, 2011. 3
- [60] Wei-Sheng Lai, Jia-Bin Huang, Narendra Ahuja, and Ming-Hsuan Yang. Deep laplacian pyramid networks for fast and accurate super-resolution. In *Proceedings of the IEEE conference on computer vision and pattern recognition*, pages 624–632, 2017. 3, 7, 8
- [61] Iro Laina, Christian Rupprecht, Vasileios Belagiannis, Federico Tombari, and Nassir Navab. Deeper depth prediction with fully convolutional residual networks. In *2016 Fourth International Conference on 3D Vision (3DV)*, pages 239–248. IEEE, 2016. 2
- [62] Jin Han Lee, Myung-Kyu Han, Dong Wook Ko, and Il Hong Suh. From big to small: Multi-scale local planar guidance for monocular depth estimation. *arXiv preprint arXiv:1907.10326*, 2019. 1, 2
- [63] Jae-Han Lee and Chang-Su Kim. Monocular depth estimation using relative depth maps. In *CVPR*, pages 9729–9738, 2019. 1, 2
- [64] Biao Li, Bo Wang, Jiabin Liu, Zhiquan Qi, and Yong Shi. s-lwsr: Super lightweight super-resolution network. *IEEE Transactions on Image Processing*, 29:8368–8380, 2020. 8
- [65] Hanchao Li, Pengfei Xiong, Haoqiang Fan, and Jian Sun. Dfanet: Deep feature aggregation for real-time semantic segmentation. In *Proceedings of the IEEE conference on computer vision and pattern recognition*, pages 9522–9531, 2019. 1, 3, 6, 7
- [66] Yunsheng Li, Yinpeng Chen, Xiyang Dai, Dongdong Chen, Mengchen Liu, Lu Yuan, Zicheng Liu, Lei Zhang, and Nuno Vasconcelos. Micronet: Improving image recognition with extremely low flops. In *Proceedings of the IEEE/CVF International Conference on Computer Vision*, pages 468–477, 2021. 4
- [67] Zhen Li, Jinglei Yang, Zheng Liu, Xiaomin Yang, Gwanggil Jeon, and Wei Wu. Feedback network for image super-resolution. In *Proceedings of the IEEE conference on computer vision and pattern recognition*, pages 3867–3876, 2019. 7, 8

- [68] Chen Liang-Chieh, George Papandreou, Iasonas Kokkinos, Kevin Murphy, and Alan Yuille. Semantic image segmentation with deep convolutional nets and fully connected crfs. In *International Conference on Learning Representations*, 2015. 3
- [69] Chen Liu, Kihwan Kim, Jinwei Gu, Yasutaka Furukawa, and Jan Kautz. Planercnn: 3d plane detection and reconstruction from a single image. In *CVPR*, pages 4450–4459, 2019. 1, 2
- [70] Chen Liu, Jimei Yang, Duygu Ceylan, Ersin Yumer, and Yasutaka Furukawa. Planenet: Piece-wise planar reconstruction from a single rgb image. In *CVPR*, pages 2579–2588, 2018. 1, 2
- [71] Chenxi Liu, Barret Zoph, Maxim Neumann, Jonathon Shlens, Wei Hua, Li-Jia Li, Li Fei-Fei, Alan Yuille, Jonathan Huang, and Kevin Murphy. Progressive neural architecture search. In *Proceedings of the European conference on computer vision (ECCV)*, pages 19–34, 2018. 3, 4
- [72] Hanxiao Liu, Karen Simonyan, and Yiming Yang. Darts: Differentiable architecture search. *arXiv preprint arXiv:1806.09055*, 2018. 3
- [73] Ze Liu, Han Hu, Yutong Lin, Zhuliang Yao, Zhenda Xie, Yixuan Wei, Jia Ning, Yue Cao, Zheng Zhang, Li Dong, et al. Swin transformer v2: Scaling up capacity and resolution. *arXiv preprint arXiv:2111.09883*, 2021. 1
- [74] Jonathan Long, Evan Shelhamer, and Trevor Darrell. Fully convolutional networks for semantic segmentation. In *Proceedings of the IEEE conference on computer vision and pattern recognition*, pages 3431–3440, 2015. 3
- [75] Renqian Luo, Fei Tian, Tao Qin, Enhong Chen, and Tiejian Liu. Neural architecture optimization. *arXiv preprint arXiv:1808.07233*, 2018. 3
- [76] Joe Mellor, Jack Turner, Amos Storkey, and Elliot J Crowley. Neural architecture search without training. In *International Conference on Machine Learning*, pages 7588–7598. PMLR, 2021. 2, 4
- [77] Hyeonwoo Noh, Seunghoon Hong, and Bohyung Han. Learning deconvolution network for semantic segmentation. In *Proceedings of the IEEE international conference on computer vision*, pages 1520–1528, 2015. 3
- [78] Marin Orsic, Ivan Kreso, Petra Bevandic, and Sinisa Segvic. In defense of pre-trained imagenet architectures for real-time semantic segmentation of road-driving images. In *Proceedings of the IEEE conference on computer vision and pattern recognition*, pages 12607–12616, 2019. 1, 3, 6, 7
- [79] Hieu Pham, Melody Guan, Barret Zoph, Quoc Le, and Jeff Dean. Efficient neural architecture search via parameters sharing. In *International Conference on Machine Learning*, pages 4095–4104. PMLR, 2018. 2, 3
- [80] Matteo Poggi, Filippo Aleotti, Fabio Tosi, and Stefano Mattoccia. Towards real-time unsupervised monocular depth estimation on cpu. In *2018 IEEE/RSJ International Conference on Intelligent Robots and Systems (IROS)*, pages 5848–5854. IEEE, 2018. 2, 6, 8, 9
- [81] Xiaojuan Qi, Renjie Liao, Zhengzhe Liu, Raquel Urtasun, and Jiaya Jia. Geonet: Geometric neural network for joint depth and surface normal estimation. In *CVPR*, pages 283–291, 2018. 2
- [82] Michael Ramamonjisoa and Vincent Lepetit. Sharpnet: Fast and accurate recovery of occluding contours in monocular depth estimation. (*ICCV Workshops*, 2019. 1, 2
- [83] René Ranftl, Alexey Bochkovskiy, and Vladlen Koltun. Vision transformers for dense prediction. *ArXiv preprint*, 2021. 1, 3
- [84] Esteban Real, Alok Aggarwal, Yanping Huang, and Quoc V Le. Regularized evolution for image classifier architecture search. In *Proceedings of the aaai conference on artificial intelligence*, volume 33, pages 4780–4789, 2019. 3, 4
- [85] Olaf Ronneberger, Philipp Fischer, and Thomas Brox. U-net: Convolutional networks for biomedical image segmentation. In *International Conference on Medical image computing and computer-assisted intervention*, pages 234–241. Springer, 2015. 3
- [86] Tonmoy Saikia, Yassine Marrakchi, Arber Zela, Frank Hutter, and Thomas Brox. Autodispnet: Improving disparity estimation with automl. In *Proceedings of the IEEE/CVF International Conference on Computer Vision*, pages 1812–1823, 2019. 2, 6
- [87] Mark Sandler, Andrew Howard, Menglong Zhu, Andrey Zhmoginov, and Liang-Chieh Chen. Mobilenetv2: Inverted residuals and linear bottlenecks. In *Proceedings of the IEEE conference on computer vision and pattern recognition*, pages 4510–4520, 2018. 3
- [88] Ashutosh Saxena, Sung H Chung, and Andrew Y Ng. Learning depth from single monocular images. In *Advances in neural information processing systems*, pages 1161–1168, 2006. 2
- [89] Nathan Silberman, Derek Hoiem, Pushmeet Kohli, and Rob Fergus. Indoor segmentation and support inference from rgb-d images. In *European Conference on Computer Vision*, pages 746–760. Springer, 2012. 5
- [90] Deqing Sun, Xiaodong Yang, Ming-Yu Liu, and Jan Kautz. Pwc-net: Cnns for optical flow using pyramid, warping, and cost volume. In *CVPR*, pages 8934–8943, 2018. 2
- [91] Ying Tai, Jian Yang, and Xiaoming Liu. Image super-resolution via deep recursive residual network. In *Proceedings of the IEEE conference on computer vision and pattern recognition*, pages 3147–3155, 2017. 3, 7, 8, 9
- [92] Ying Tai, Jian Yang, Xiaoming Liu, and Chunyan Xu. Memnet: A persistent memory network for image restoration. In *Proceedings of the IEEE international conference on computer vision*, pages 4539–4547, 2017. 1, 7, 8
- [93] Mingxing Tan, Bo Chen, Ruoming Pang, Vijay Vasudevan, Mark Sandler, Andrew Howard, and Quoc V Le. Mnasnet: Platform-aware neural architecture search for mobile. In *CVPR*, pages 2820–2828, 2019. 4
- [94] Xiaohan Tu, Cheng Xu, Siping Liu, Renfa Li, Guoqi Xie, Jing Huang, and Laurence Tianruo Yang. Efficient monocular depth estimation for edge devices in internet of things. *IEEE Transactions on Industrial Informatics*, 17(4):2821–2832, 2020. 2, 3, 6, 8, 11
- [95] Jingdong Wang, Ke Sun, Tianheng Cheng, Borui Jiang, Chaorui Deng, Yang Zhao, Dong Liu, Yadong Mu, Mingkui

- Tan, Xinggang Wang, et al. Deep high-resolution representation learning for visual recognition. *IEEE transactions on pattern analysis and machine intelligence*, 2020. [1](#), [3](#), [6](#)
- [96] Diana Wofk, Fangchang Ma, Tien-Ju Yang, Sertac Karaman, and Vivienne Sze. Fastdepth: Fast monocular depth estimation on embedded systems. In *2019 International Conference on Robotics and Automation (ICRA)*, pages 6101–6108. IEEE, 2019. [1](#), [2](#), [3](#), [6](#), [8](#), [9](#), [11](#)
- [97] Bichen Wu, Xiaoliang Dai, Peizhao Zhang, Yanghan Wang, Fei Sun, Yiming Wu, Yuandong Tian, Peter Vajda, Yangqing Jia, and Kurt Keutzer. Fbnet: Hardware-aware efficient convnet design via differentiable neural architecture search. In *Proceedings of the IEEE conference on computer vision and pattern recognition*, pages 10734–10742, 2019. [6](#), [8](#), [11](#)
- [98] Guanglei Yang, Hao Tang, Mingli Ding, Nicu Sebe, and Elisa Ricci. Transformers solve the limited receptive field for monocular depth prediction. *arXiv preprint arXiv:2103.12091*, 2021. [1](#), [3](#)
- [99] Tien-Ju Yang, Andrew Howard, Bo Chen, Xiao Zhang, Alec Go, Mark Sandler, Vivienne Sze, and Hartwig Adam. Netadapt: Platform-aware neural network adaptation for mobile applications. In *Proceedings of the European Conference on Computer Vision (ECCV)*, pages 285–300, 2018. [1](#), [3](#)
- [100] Wenming Yang, Wei Wang, Xuechen Zhang, Shuifa Sun, and Qingmin Liao. Lightweight feature fusion network for single image super-resolution. *IEEE Signal Processing Letters*, 26(4):538–542, 2019. [7](#), [8](#)
- [101] Wei Yin, Yifan Liu, Chunhua Shen, and Youliang Yan. Enforcing geometric constraints of virtual normal for depth prediction. In *The IEEE International Conference on Computer Vision (ICCV)*, 2019. [2](#)
- [102] Changqian Yu, Changxin Gao, Jingbo Wang, Gang Yu, Chunhua Shen, and Nong Sang. Bisenet v2: Bilateral network with guided aggregation for real-time semantic segmentation. *International Journal of Computer Vision*, 129(11):3051–3068, 2021. [6](#), [7](#)
- [103] Changqian Yu, Jingbo Wang, Chao Peng, Changxin Gao, Gang Yu, and Nong Sang. Bisenet: Bilateral segmentation network for real-time semantic segmentation. In *Proceedings of the European conference on computer vision (ECCV)*, pages 325–341, 2018. [3](#), [6](#), [7](#)
- [104] Changqian Yu, Bin Xiao, Changxin Gao, Lu Yuan, Lei Zhang, Nong Sang, and Jingdong Wang. Lite-hrnet: A lightweight high-resolution network. In *Proceedings of the IEEE conference on computer vision and pattern recognition*, pages 10440–10450, 2021. [1](#), [6](#), [7](#), [8](#)
- [105] Mehmet Kerim Yucel, Valia Dimaridou, Anastasios Drosou, and Albert Saa-Garriga. Real-time monocular depth estimation with sparse supervision on mobile. In *Proceedings of the IEEE conference on computer vision and pattern recognition*, pages 2428–2437, 2021. [3](#), [6](#)
- [106] Roman Zeyde, Michael Elad, and Matan Protter. On single image scale-up using sparse-representations. In *International conference on curves and surfaces*, pages 711–730. Springer, 2010. [8](#)
- [107] Yulun Zhang, Kunpeng Li, Kai Li, Lichen Wang, Bineng Zhong, and Yun Fu. Image super-resolution using very deep residual channel attention networks. In *Proceedings of the European conference on computer vision (ECCV)*, pages 286–301, 2018. [3](#)
- [108] Hengshuang Zhao, Xiaojuan Qi, Xiaoyong Shen, Jianping Shi, and Jiaya Jia. Icnnet for real-time semantic segmentation on high-resolution images. In *Proceedings of the European conference on computer vision (ECCV)*, pages 405–420, 2018. [3](#), [6](#), [7](#)
- [109] Hengshuang Zhao, Jianping Shi, Xiaojuan Qi, Xiaogang Wang, and Jiaya Jia. Pyramid scene parsing network. In *Proceedings of the IEEE conference on computer vision and pattern recognition*, pages 2881–2890, 2017. [2](#), [3](#)
- [110] Shuai Zheng, Sadeep Jayasumana, Bernardino Romera-Paredes, Vibhav Vineet, Zhizhong Su, Dalong Du, Chang Huang, and Philip HS Torr. Conditional random fields as recurrent neural networks. In *Proceedings of the IEEE international conference on computer vision*, pages 1529–1537, 2015. [3](#)
- [111] Daquan Zhou, Qibin Hou, Yunpeng Chen, Jiashi Feng, and Shuicheng Yan. Rethinking bottleneck structure for efficient mobile network design. In *Computer Vision—ECCV 2020: 16th European Conference, Glasgow, UK, August 23–28, 2020, Proceedings, Part III 16*, pages 680–697. Springer, 2020. [6](#)
- [112] Feiyang Zhu and Qijun Zhao. Efficient single image super-resolution via hybrid residual feature learning with compact back-projection network. In *Proceedings of the IEEE/CVF International Conference on Computer Vision Workshops*, pages 0–0, 2019. [7](#), [8](#)
- [113] Barret Zoph and Quoc V Le. Neural architecture search with reinforcement learning. *arXiv preprint arXiv:1611.01578*, 2016. [1](#), [3](#)
- [114] Barret Zoph, Vijay Vasudevan, Jonathon Shlens, and Quoc V Le. Learning transferable architectures for scalable image recognition. In *Proceedings of the IEEE conference on computer vision and pattern recognition*, pages 8697–8710, 2018. [1](#), [3](#), [4](#)